Supporting Information

Self-assembly of anionic, ligand-coated nanoparticles in lipid membranes

Panagiotis Angelikopoulos Lev Sarkisov, Zoe Cournia and Paraskevi Gkeka

A. Nanoparticle description

The nanoparticle (NP) used in the present study is presented in Figure S1. It has a core diameter of 3 nm coated with regular, striped patterns of hydrophobic (octanethiol, OT) and negatively charged (11-mercapto-1-undecanesulphonate, MUS) domains in a 1:1 MUS:OT ratio. The NP has in total 271 attached ligands out of which 134 have a negatively charged terminal, represented by the Qa MARTINI particle type that carries a net charge of -1e.

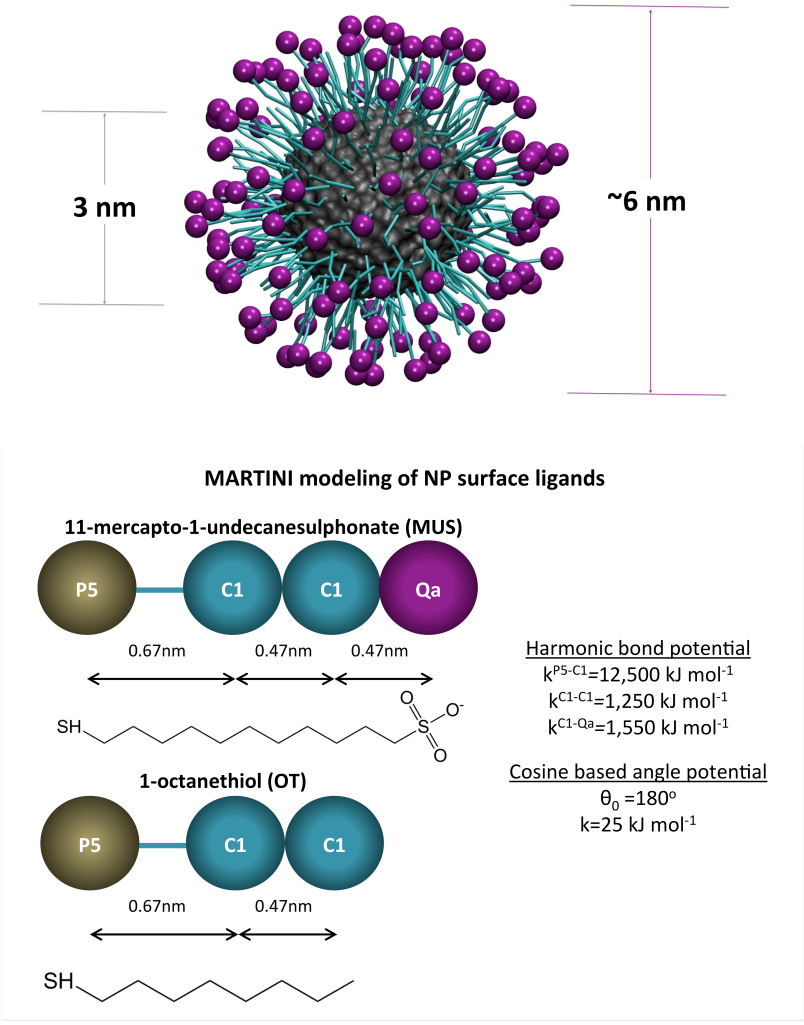

Figure S1. Coarse-grained representation of the NP used in the present study (top). Model of the NP surface ligands (bottom). Colors: Negative particles bearing -1e charge (Qa) = purple; hydrophobic particles (C1) = cyan; and polar particles (P5) = ochre.

B. Systems and simulations summary

Table S1. Summary of simulations with the anionic, ligand-coated NPs.

<table>
<tr><th></th><th>0% mol. cholesterol</th><th>30% mol. cholesterol</th></tr>
<tr><td rowspan="2">2 NPs</td><td>System 1.2
14.6 μs
No cluster formed.</td><td rowspan="2">System 2.2
12.0 μs
Dimer formation.</td></tr>
<tr><td>System 1.2*
6.0 μs
Preformed dimer.</td></tr>
<tr><td rowspan="2">3 NPs</td><td rowspan="2">System 1.3
15.5 μs
No cluster formed.</td><td>System 2.3
15.2 μs
Starting configuration with a dimer and a monomer in the bilayer. Linear trimer formation.</td></tr>
<tr><td>System 2.3*
10.0 μs
Preformed trimer in a triangular structure.</td></tr>
<tr><td rowspan="3">4 NPs</td><td rowspan="3">System 1.4
15.3 μs
No cluster formed.</td><td>System 2.4A
19.4 μs
Linear tetramer formation.</td></tr>
<tr><td>System 2.4B
10.1 μs
Two NPs originally at a closer distance. Linear trimer formation.</td></tr>
<tr><td>System 2.4*
10.0 μs
Preformed tetramer in square-like structure.</td></tr>
</table>

C. Dimer formation by anionic, ligand-coated NPs

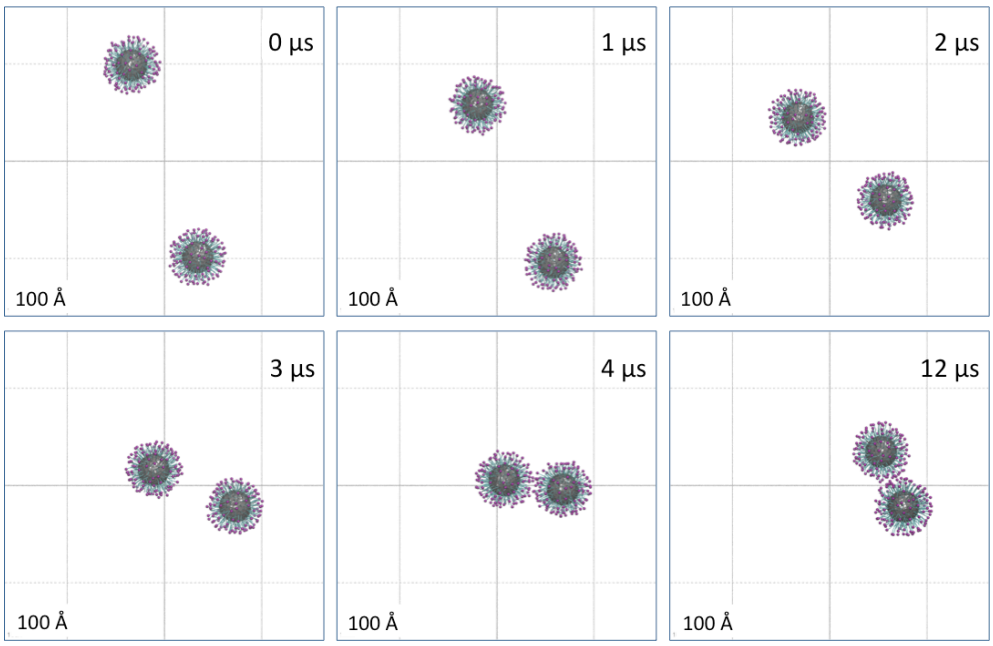

Figure S2. Top view snapshots of the dimer formation in a lipid bilayer containing 30% mol. cholesterol. The NP core is shown as grey surface, NP ligand hydrophobic tails are shown in licorice representation colored in cyan, polar NP ligand termini are shown as purple particles. The rest of the system components are not shown for clarity.

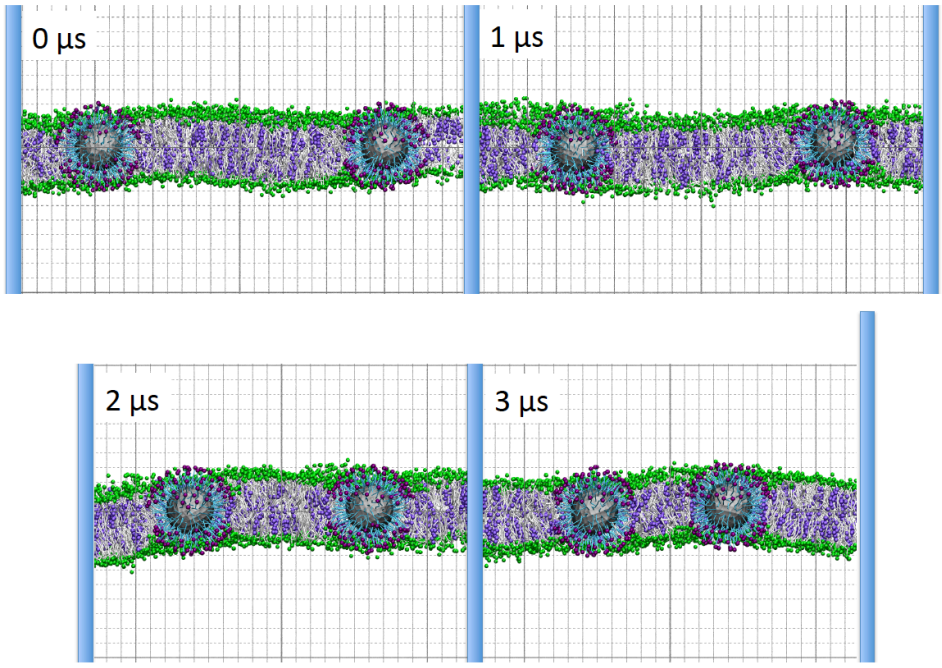

Figure S3. Side view snapshots of the dimer formation in a lipid bilayer containing 30% mol. cholesterol. The NP core is shown as grey surface, NP ligand hydrophobic tails are shown in licorice representation colored in cyan, polar NP ligand termini are shown as purple particles. Lipid tails are shown in white licorice representation. DPPC lipid heads (NC3 and PO4 groups) are shown as green particles Cholesterol is represented as mauve particles. Water and ions are not shown for clarity.

D. NP-NP distance as a function of time - NP self-assembly in the cholesterol-containing bilayer

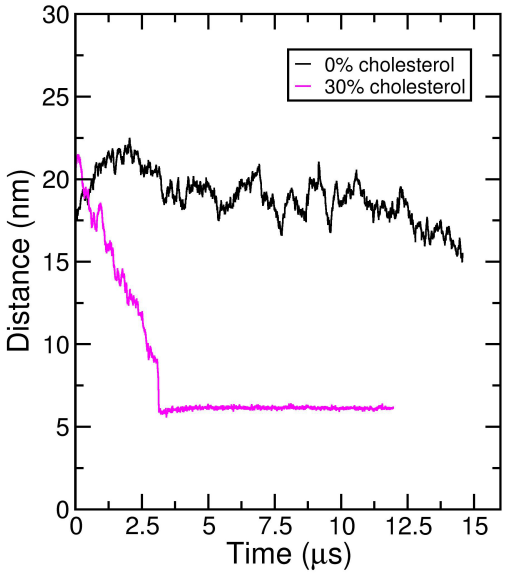

Figure S4. NP-NP center-of-mass distances for the two-nanoparticle system and for the 0% and 30% mol. cholesterol cases.

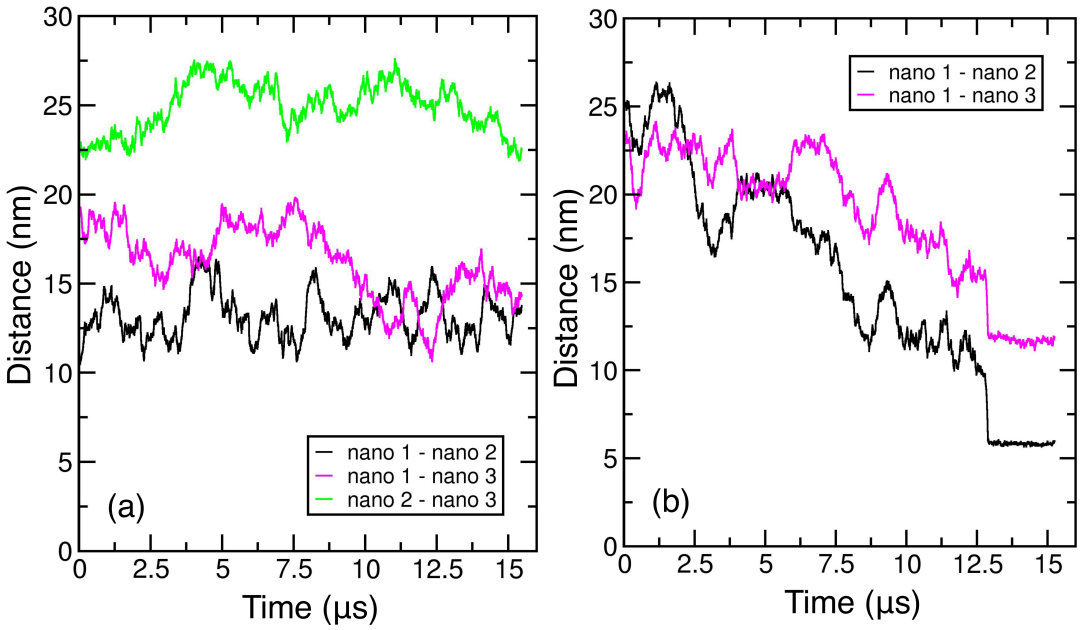

Figure S5. NP-NP center-of-mass distances for the three NP system and for the 0% (left) and 30% (right) mol. cholesterol cases.

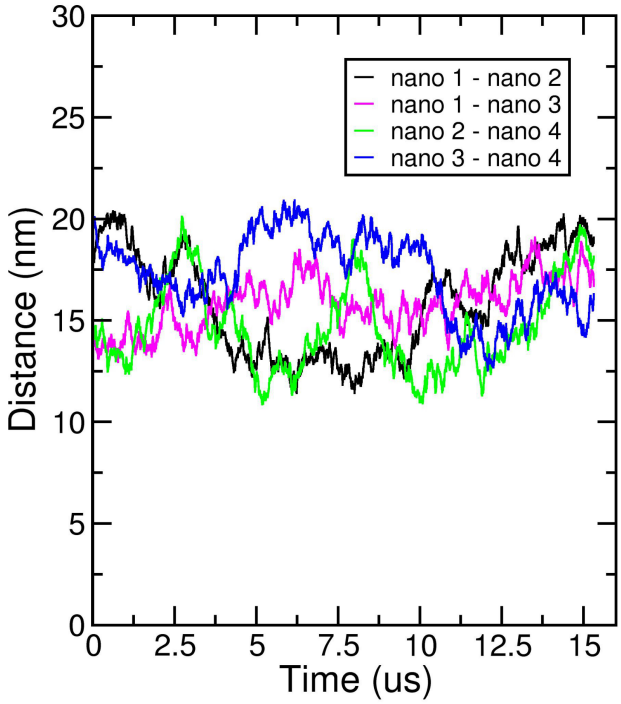

Figure S6. NP-NP center-of-mass distances for the four NP system in the cholesterol-free lipid bilayer.

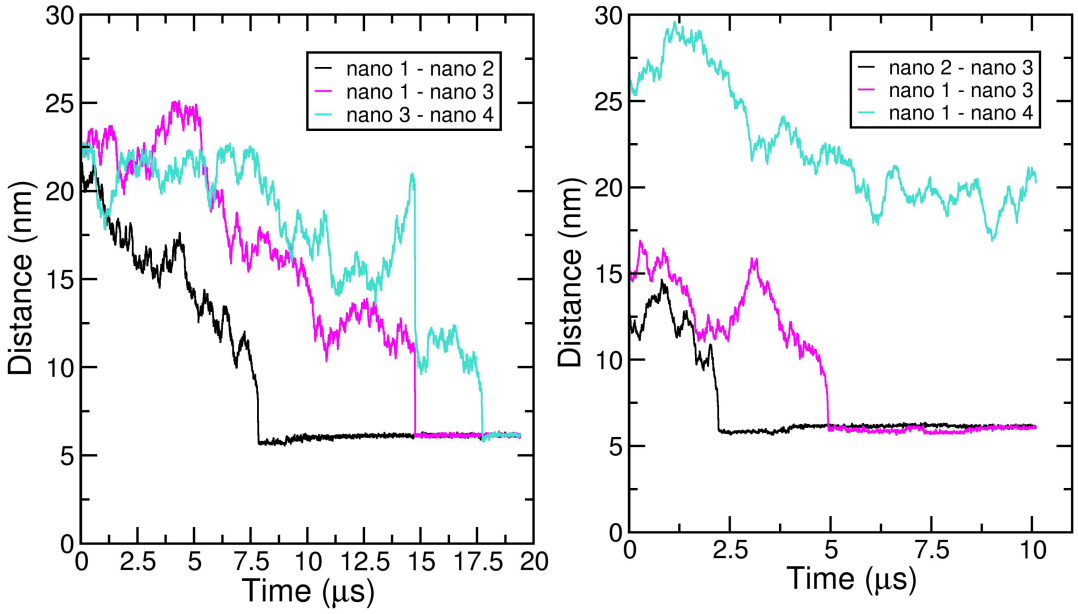

Figure S7. NP-NP center-of-mass distances for the four NP systems and the 30% mol. cholesterol. Left: Formation of tetramer is observed in simulation #1. Right: A trimer is formed in simulation #2.

E. Analysis of the NP tetramer in the cholesterol containing bilayer

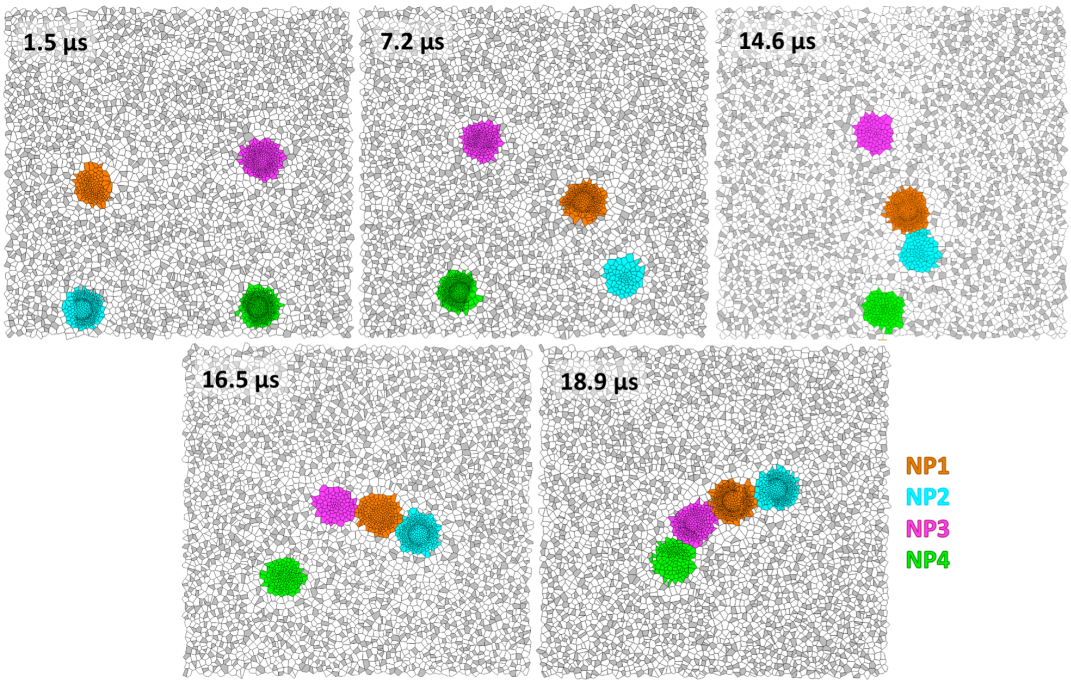

Figure S8. Snapshots in Voronoi representation from the simulation of four anionic NPs in a lipid bilayer containing 30% cholesterol. Cholesterol is shown in grey and each of the four NPs is colored differently to show its relative position during the formation of the tetramer.

In Figure S9, we present the final snapshot of the tetramer NP association. A change from a thickness of 4.5 nm (in the bulk membrane) to 2.0 nm (in the area close to the NPs) indicates a significant hydrophobic mismatch

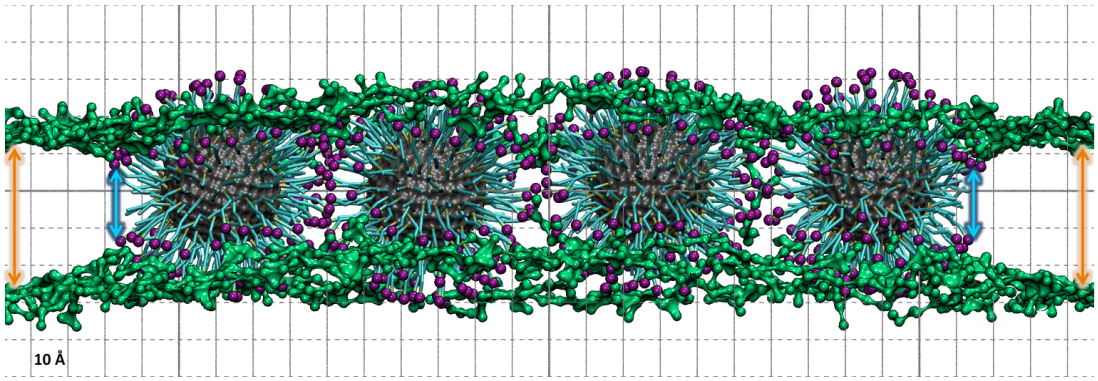

Figure S9. Final snapshot from the simulation of the tetramer formation (system 2.4A from Table S1). Hydrophobic length mismatch between the lipid bilayer core and NP hydrophobic ligand tails is depicted as blue arrows while bulk lipid bilayer thickness is depicted with orange double arrows. DPPC lipid heads (NC3 and PO4 groups) = green surface, NP core = grey surface, NP ligand hydrophobic tails = licorice representation colored in cyan, polar NP ligand ends = purple VDW spheres. Water, ions, cholesterol, and the hydrophobic lipid tails are not shown for clarity.

In Figure S10, we present the evolution of the lipid bilayer thickness for System 2.4A (see Table S1).

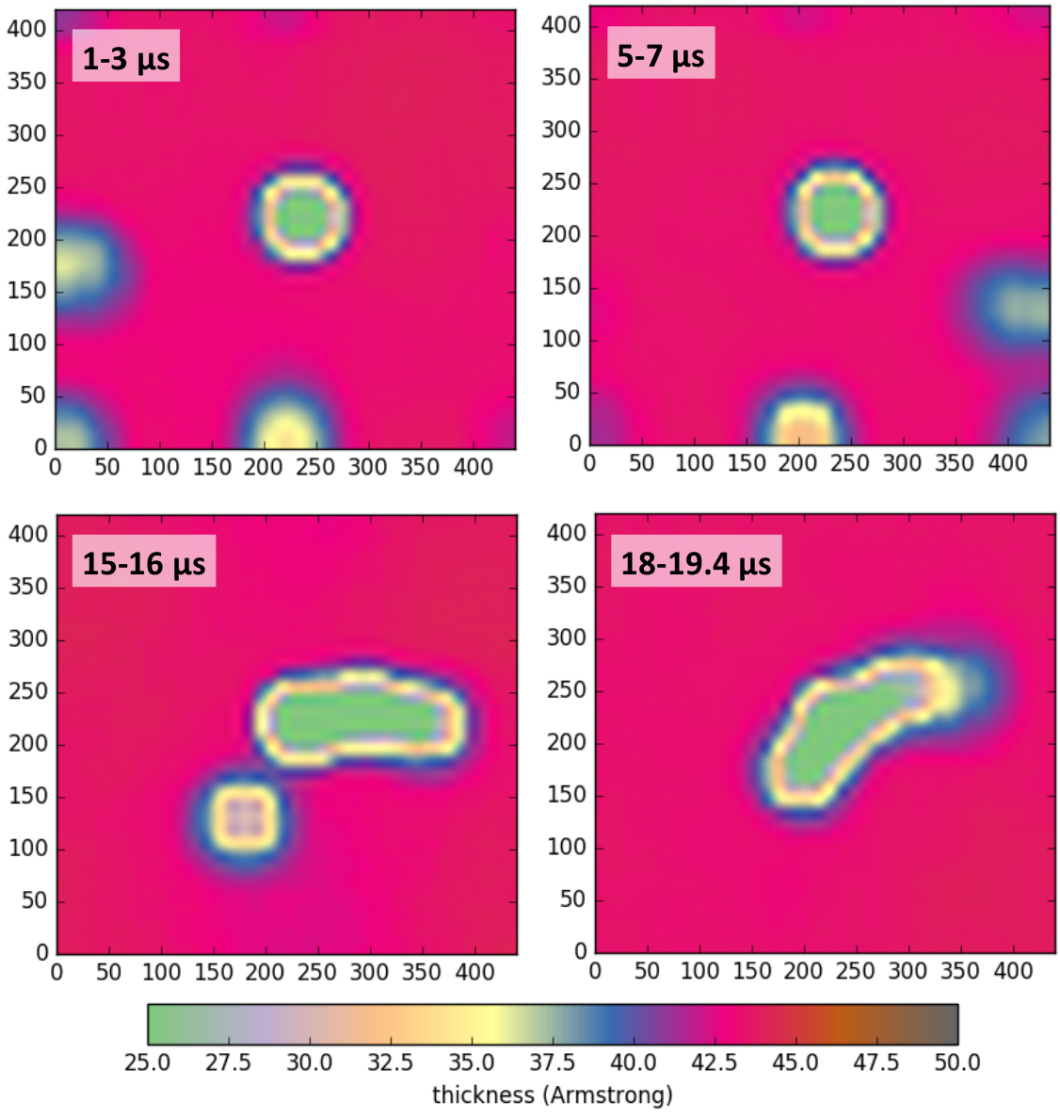

Figure S10. Evolution of lipid bilayer thickness for the system containing a bilayer with 30% mol. cholesterol and four NP inclusions, which form a linear tetramer (System 2.4A, Table S1).

F. Geometric analysis of liquid-ordered and liquid-disordered domains

Consider a process of two NPs, forming a dimer as schematically depicted in Figure S11. The red line delineates a boundary between two domains. The region in the vicinity of the NPs, shown in blue, is characterized by the lower cholesterol concentration, lower bilayer thickness and greater disorder (it is in the liquid-disordered phase). The remaining bilayer, outside of the region enclosed by the red line, is characterized by higher cholesterol concentration, larger bilayer thickness and higher structural order (it is in the liquid-ordered phase).

In this geometric analysis we are interested in two primary geometric characteristics, the circumference of the boundary between the two domains (the length of the red line), L, and the area of the domain enclosed within the red line, S. The analysis provides expressions for the values of these characteristics as a function of the distance between the two NPs.

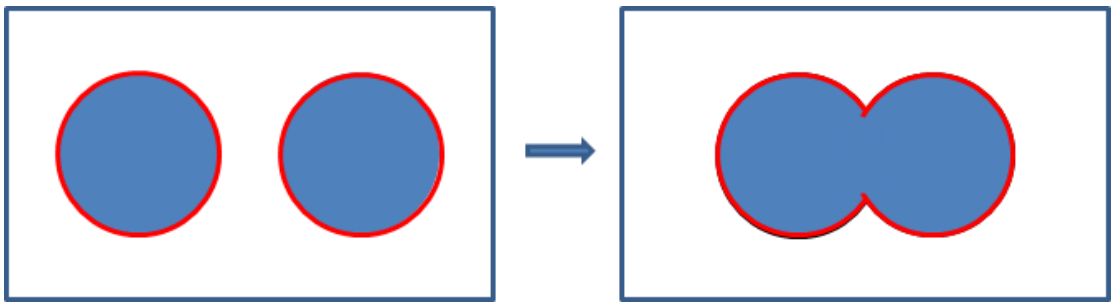

Figure S11. Schematic illustration of the dimerization process between two NPs as seen from the perspective normal to the lipid bilayer plane. Blue areas correspond to the regions in the vicinity of the NPs, with structural characteristics of the bilayer affected by the presence of the NP; at the distances greater than those demarcated by the red line, bilayer attains bulk characteristics.

First, we define some variables associated with the geometry of system. We treat the liquid-disordered phase around an NP as a circular area of radius r (red circles in Figure S12).

$L_0 = 2 \cdot 2\pi r$ is the circumference of the liquid-disordered domain at the beginning of the process, with two NPs not yet associated (the circumference associated with one NP times two).

$S_0 = 2 \cdot \pi r^2$ is the area of the liquid-disordered domain at the beginning of the process, with two NPs not yet associated (the area of blue circle times two)

D is the distance separating two NPs.

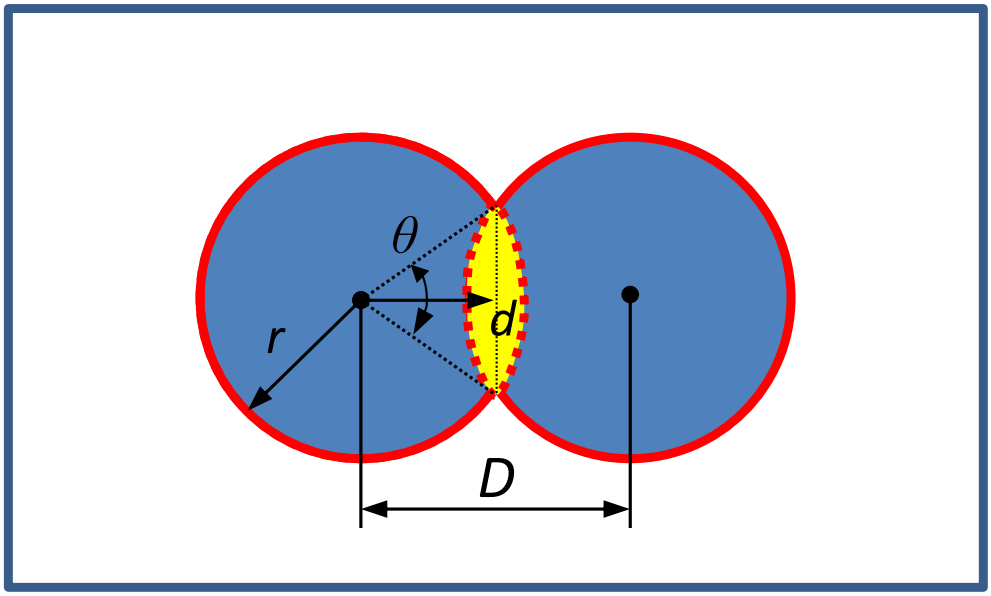

Figure S12. Geometry of the dimer. Upon dimer formation, the circumference of the liquid-disordered domain reduces by the length of two arcs shown in red dashed lines; the area of the liquid-disordered domain is reduced by the value equivalent to the yellow area in the figure.

As can be seen from Figure S12, upon forming the dimer, L is reduced by the length of two arcs shown in dashed red lines, while S is reduced by the area shown in Figure S15 in yellow colour, compared to the initial values. Thus, to calculate $L = f(D)$ and $S = f(D)$ we need basic geometric formulae for the arc length and area of segment. Geometric properties necessary for these calculations are defined in Figure S12.

From the basic geometry, the length of the arc as shown is:

$l_{arc} = \theta r$, where $\theta = 2arccos\left(\frac{d}{r}\right)$ (1)

and, the area of the segment as shown (half of the yellow region) is:

$s_{seg} = \frac{r^2}{2}(\theta - sin\theta)$ (2)

Expressed through the distance between the centers of the NPs (see Figure 2):

$d = D/2$, so $\theta = 2arccos\left(\frac{D}{2r}\right)$ (3)

Therefore, upon forming a dimer, the new values of L and S are:

$L_1 = L_0 - 2 \cdot l_{arc} = 4\pi r - 4r \cdot arccos\left(\frac{D}{2r}\right)$ (4)

$S_1 = S_0 - 2 \cdot s_{seg} = 2\pi r^2 - r^2 \cdot \left[2arccos\left(\frac{D}{2r}\right) - sin\left(2arccos\left(\frac{D}{2r}\right)\right)\right]$ (5)

To study the behaviour of these properties during dimer formation, we can consider the values of the term $\frac{D}{2r}$ from 1 (the two blue circles just touched) to 0.5 (two blue circles are at distance r from each other), although the lower boundary is not realistic in the context of NP association.

$L/L_0 = f(\frac{D}{2r})$ and $S/S_0 = f(\frac{D}{2r})$ are shown in Figure S13; indeed upon association the circumference and the area associated with the liquid-disordered domain around NPs are reduced.

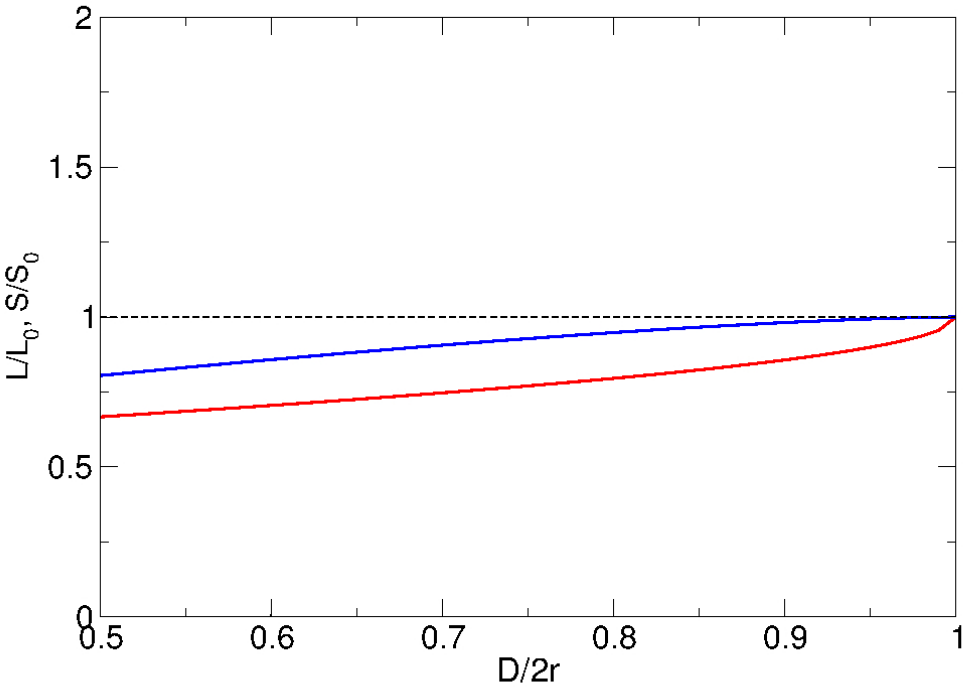

Figure S13. Dimensionless circumference (red) and area (blue) of the liquid-disordered domain around NPs as a function of dimensionless distance. D/2r=1 corresponds to the two NPs in the initial, monomer state.

Now in the second leg of the analysis we consider a situation where, upon forming a dimer, the disordered area around NPs increases in size (due to some cooperative effects). This is schematically depicted in Figure S14 and this expansion can be modelled by scaling the initial radius of the blue circles by some factor f.

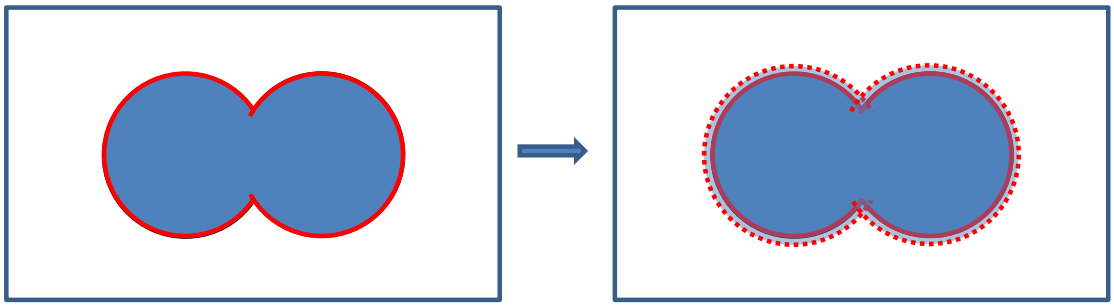

Figure S14. Schematic depiction of the expansion of the size of liquid-disordered domain around the NPs, upon the dimer formation.

In this case, formulae similar to Eqs 1-5 can be applied to calculate the circumference and the area of the disordered domain:

$$L_2 = 4\pi fr - 4r \cdot arccos\left(\frac{D}{2fr}\right) \qquad (6)$$

$$S_2 = 2\pi(fr)^2 - (fr)^2 \cdot \left[2arccos\left(\frac{D}{2fr}\right) - sin\left(2arccos\left(\frac{D}{2fr}\right)\right)\right] \qquad (7)$$

Again, we are interested in how these properties compare to the initial values, L_0, S_0, before the association. These are shown in Figure S15 for $f = 1.1$ as a case study.

As can be seen from the figure, comparing to the initial values, the area increases, while the circumference is reduced. This implies that if the driving forces associated with the line tension between the two domains dominate over the forces associated with the surface tension within the liquid-disordered domain, the NPs are driven to associate with each other even if it may lead to an increase in the size of the liquid-disordered domain, as long as its circumference is reduced.

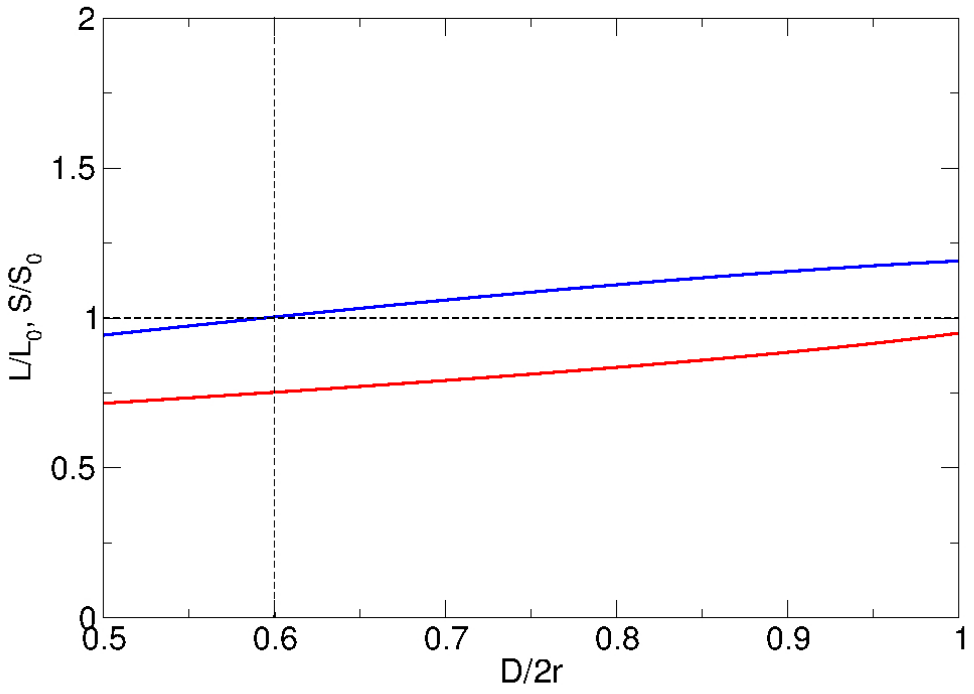

Figure S15. Dimensionless circumference (red) and area (blue) of the liquid-disordered domain around NPs as a function of dimensionless distance in the process where dimerization is followed by the expansion of the liquid disordered domain (*f*=1.1). *D/2r*=1 corresponds to the two NPs in the initial, monomer state. The horizontal dashed line corresponds to the initial reference state of the system, L_0, S_0. The vertical dashed line separates the range of *D/2r* values into the range where both L, S are lower than the initial values (to the left of the dashed line) and the range where $L<L_0$, while $S>S_0$ (to the right of the dashed line)

G. Geometry of the NP clusters

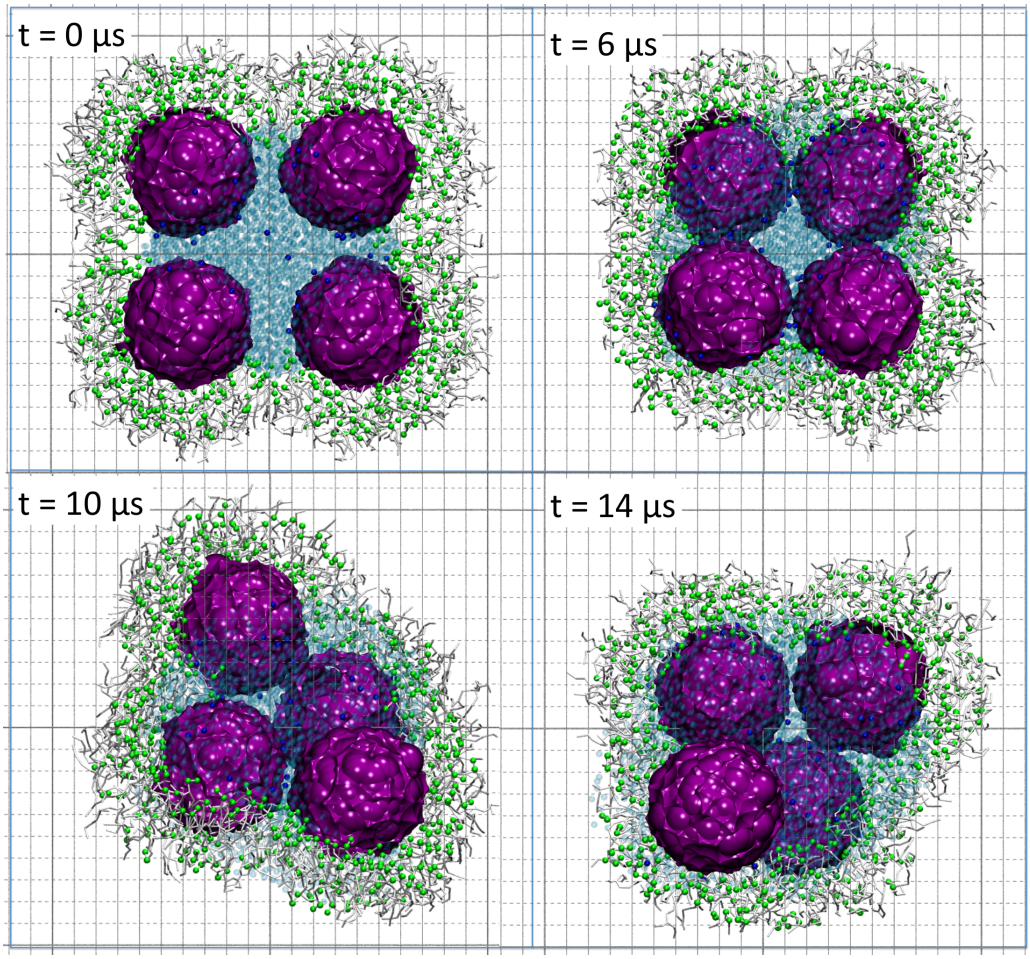

Figure S16. Snapshots from the simulation of the preformed non-linear tetramer (top view). DPPC lipid heads (NC3 and PO4 groups) = green VMD spheres, DPPC hydrophobic tails = licorice representation colored in white, polar NP ligand ends = purple surface. Water is shown as transparent blue VDW spheres. The rest of the system's components are not shown for clarity.

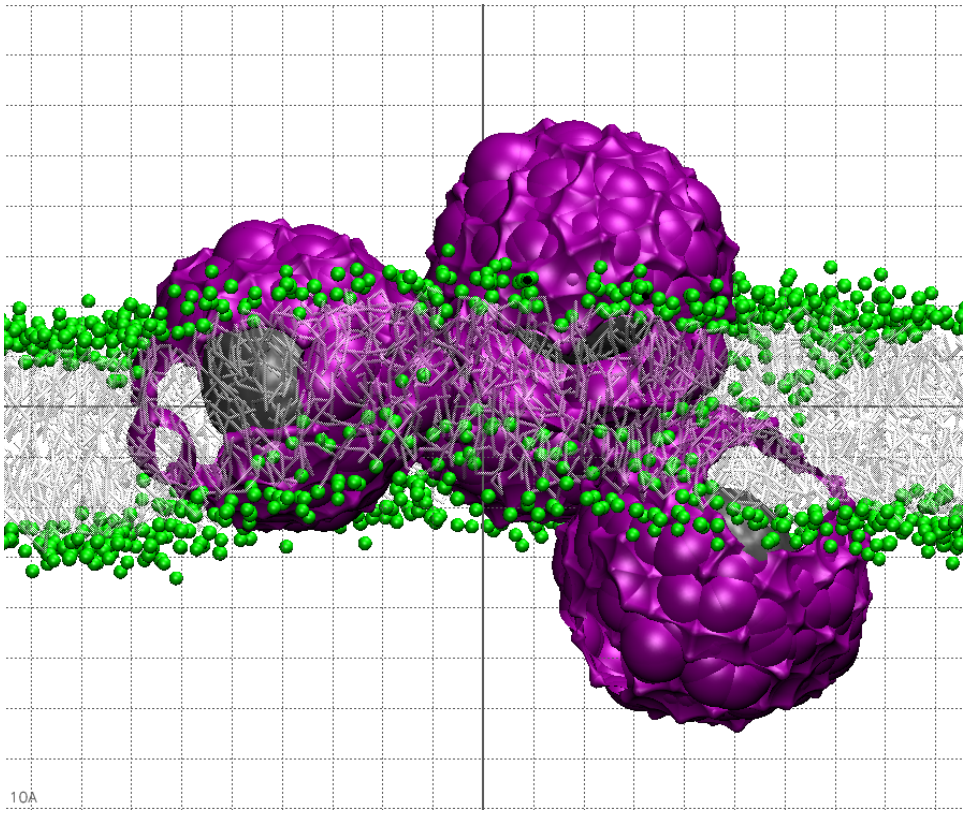

Figure S17. Final snapshot from the simulation of the preformed non-linear tetramer (side view). The representation of system components is the same as in Figure S16.

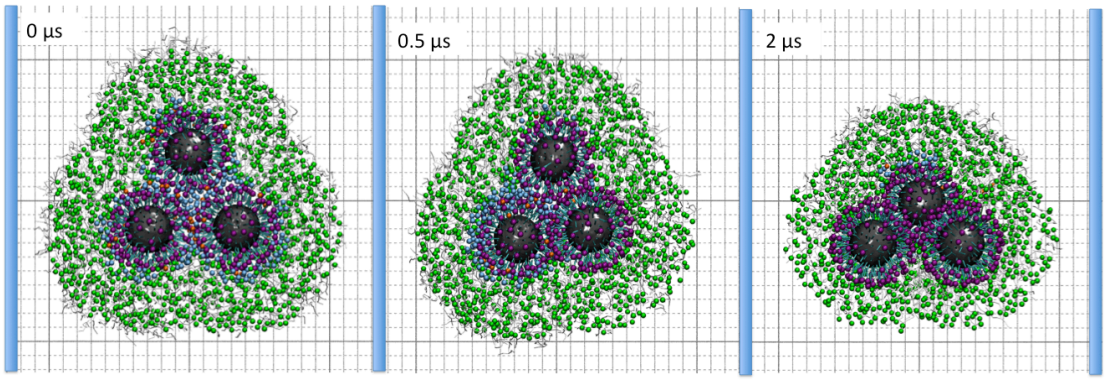

Figure S18. Snapshots from the simulation of the preformed non-linear trimer (top view). DPPC lipid heads (NC3 and PO4 groups) = green VMD spheres, DPPC hydrophobic tails = licorice representation colored in white, polar NP ligand ends = purple VDW spheres. Water is shown as transparent blue VDW spheres. The rest of the system's components are not shown for clarity.

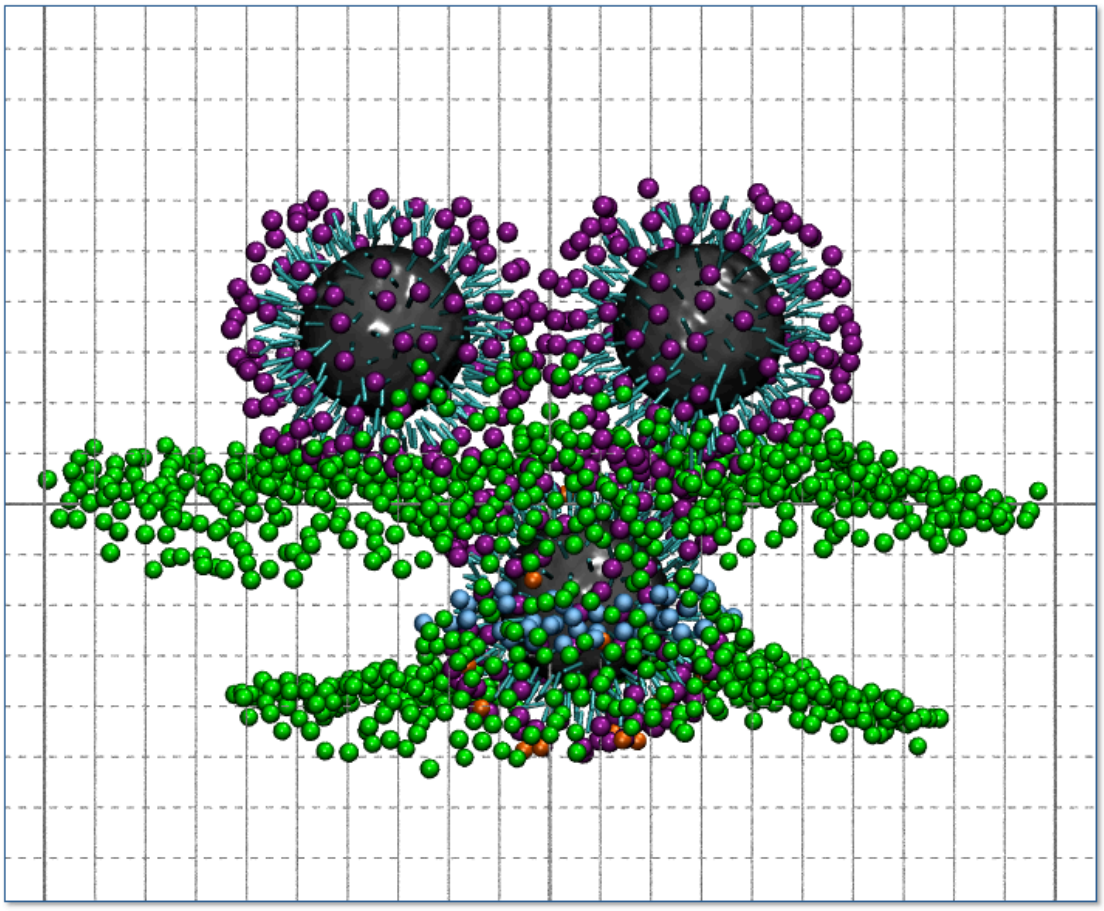

Figure S19. Final snapshot from the simulation of the preformed non-linear trimer (side view). The representation of system components is the same as in Figure S18.